



# The asset of ultra-fast digitizers for positron-lifetime spectroscopy

F. Bečvář\*, J. Čížek, I. Procházka, J. Janotová

*Department of Low-Temperature Physics, Faculty of Mathematics and Physics, Charles University, V Holešovičkách 2, CZ-180 00 Prague 8, Czech Republic*

Received 7 July 2004; received in revised form 7 September 2004; accepted 23 September 2004  
Available online 30 October 2004

## Abstract

A spectrometer for positron-lifetime measurements assembled from two BaF<sub>2</sub> scintillation detectors and two 8-bit, 4GS<sup>-1</sup> digitizes in a master–slave configuration is described in detail. We report the results of comparative testing measurements of the lifetime of positrons annihilating in  $\alpha$ -Fe using this setup and a setup formed by the same pair of detectors working in conjunction with analog electronics modules. The data from these measurements demonstrate for the first time that replacing the analog electronics chain by fast digitizers leads to a substantial improvement of the precision in positron-lifetime measurements. A record timing resolution of 131–136 ps has been achieved with the described spectrometer at coincidence counting rate comparable or virtually equal to that obtained with the fast–fast setup.

© 2004 Elsevier B.V. All rights reserved.

PACS: 78.70.Bj; 29.40.Mc; 29.30.Kv; 84.30.Sk; 85.60.Ha

**Keywords:** Positron annihilation in condensed matter; Positron-lifetime spectroscopy; BaF<sub>2</sub> scintillators; Fast digitizers; Timing resolution power; Photomultipliers

## 1. Introduction

The positron-lifetime spectroscopy proved to be a very efficient tool for the study of the micro-structure of a broad class of condensed-matter systems. However, in spite of the innovations that

this technique underwent during the last two decades, in some respect it still stagnates as it suffers from a persisting problem of a limited timing resolution. The need for substantial improvement of this important characteristic is exceptionally strong while studying lifetimes of positrons annihilating in metallic systems with a high defect concentration. Indeed, the lifetime of free positrons in such systems is shortened down to several tens of picoseconds [1], whereas a typical

\*Corresponding author. Tel.: +420 2 2191 2566; fax: +420 2 2191 2567.

E-mail address: [becvar@mbox.troja.mff.cuni.cz](mailto:becvar@mbox.troja.mff.cuni.cz) (F. Bečvář).

timing resolution of a vast majority of positron-lifetime spectrometers is characterized by a FWHM of 200 ps or higher. But an improvement of timing resolution is of utmost importance also for a large number of other applications of positron-lifetime spectroscopy.

Since the first successful use of an ultra-fast eight-bit digitizer in a setup for positron-lifetime measurements [2,3] another paper devoted to this innovative approach has recently appeared [4] and very promising results have been achieved. In particular, as seen from Ref. [4], with a triple-coincidence setup, incorporating the fast LeCroy Wavepro 950 digital oscilloscope and  $\gamma$  detectors, formed by BaF<sub>2</sub> scintillators and fast Hamamatsu H3378 photomultiplier tubes (PMTs), timing resolution power, represented by FWHM of 118.5 ps, has been reached in the measurement of the parapositronium lifetime in  $\alpha$ -SiO<sub>2</sub> with the <sup>22</sup>Na positron source. With the same setup working in the two-detector mode of operation the FWHM characterizing the achieved timing resolution power was 144 ps.

In spite of a number of unquestionable advantages of the digital processing technique, as summarized in Ref. [2], it is not yet clear whether the timing resolution power achieved with the ultra-fast digitizers is indeed better compared to that obtained using the conventional electronics systems based on the use of constant-fraction discriminators in conjunction with time-to-analog converters (TACs) and analog-to-digital converters (ADCs). So far, no solid, thoroughgoing study has been undertaken to clarify this point. In the literature one can find only a laconic statement that the performance of the digital processing technique is close to that typically obtained with analog pulse processing electronics [2].

If the systems employing the ultra-fast digitizers turn out to be superior, another question that needs an answer is whether a finite sampling rate and the 8-bit precision of the up-to-date ultra-fast digitizers together with the way in which the digitized detector signals are processed are not factors that still represent a hurdle in full exploitation of the excellent timing properties of BaF<sub>2</sub> scintillators. However, these issues will be a subject of our separate paper.

In order to assess whether the introduction of ultra-fast digitizers brings, indeed, a marked progress in positron-lifetime spectroscopy, we have performed comparative measurements of lifetimes of positrons in a well-studied system of  $\alpha$ -Fe employing separately a conventional fast-fast electronics setup and a setup including a pair of 8-bit, 4 GS s<sup>-1</sup> Acqiris DC-241 digitizers.<sup>1</sup> The data accumulated from these measurements made us possible to ascertain the real asset of the digital positron-lifetime spectroscopy. It was vitally important that these measurements were done under equal conditions, using the same pair of BaF<sub>2</sub> scintillation detectors.

## 2. The positron source, sample and detectors used for testing

The above-outlined measurements of positron-lifetime spectra were undertaken using a carrier-free <sup>22</sup>Na positron source with activity of 1 MBq sandwiched between two 0.5 mm thick disks of well-annealed  $\alpha$ -Fe. The method we used for the preparation of the <sup>22</sup>Na source is described elsewhere [5].

For all measurements we employed two  $\gamma$ -ray detectors described in detail in Ref. [5]. The detectors were formed by cylindrical BaF<sub>2</sub> crystals of size 25 mm in diameter and 10 mm in height coupled to the quartz-window Philips XP-2020/Q PMTs. The crystals were polished. Their front and side surfaces were coated with seven layers of PTFE (Teflon) tape with a thickness of 38  $\mu$ m and a pore size of 0.22  $\mu$ m. Non-standard voltage dividers were used to achieve an optimum timing resolution. They are described in Ref. [5], where they are referred to as “Dividers IV”. The high voltage applied between the photocathode and the grounded dynode No. 11 was adjusted to  $-2700$  V; with this adjustment the voltage between the dynode No. 1 and the photocathode was 900 V. The need for applying this extremely high voltage has been corroborated in Ref. [6]. Following the recommendation in Ref. [7], the detector signals

<sup>1</sup>By courtesy of Acqiris, SA, Geneva these instruments had been at our disposal for temporary use.

were extracted from the dynode No. 10. Both detectors were assembled in 1993 and they have been used almost continuously for positron-lifetime measurements for more than 10 years. Throughout this period the dividers, PMTs, BaF<sub>2</sub> crystals and even the optical coupling between the PMTs and the crystals were intact.

In order to minimize the uncertainty of electron transit time from the photocathode to the first dynode, the local magnetic field at the site where the PMTs were situated was carefully compensated with the aid of Helmholtz coils.

A close face-to-face detector geometry with a common symmetry axis was chosen. To minimize the parasitic effects of simultaneous detections of both annihilation 511.0 keV photons the sandwiched <sup>22</sup>Na source was located out of the detector axis at a radial distance slightly greater than the radius of the BaF<sub>2</sub> crystals. In order to suppress the detector cross-talk caused by the  $\gamma$ -ray scattering from the BaF<sub>2</sub> crystals, a 2 mm Pb sheet has been inserted between them.

### 3. Testing measurements

In all our measurements with the setup employing the DC-241 digitizers and the setup formed by the fast–fast electronics system one of the detectors—the “start” detector—served for detecting the 1274.6 keV nuclear  $\gamma$ -ray, depopulating the short-lived ( $\tau = 3.7$  ps) 1274.6 keV level of the daughter <sup>22</sup>Ne nucleus, while the other detector—the “stop” detector—served for detection of one of the 511.0 keV  $\gamma$ -rays, originating from positron annihilation. As the 1274.6 keV level in <sup>22</sup>Ne is populated virtually at the moment of a birth of a positron, the time difference between detections of the annihilation and nuclear  $\gamma$ -rays may serve for determining the age of a positron. The central problem of positron-lifetime spectroscopy is to choose the  $\gamma$  detectors that produce signals with excellent timing properties and to elaborate the method that makes it possible to extract, from these signals, the detection-time difference with a maximum precision.

### 3.1. The measurement with Acqiris DC-241 digitizers

#### 3.1.1. The setup and the measurement itself

The block scheme of the setup incorporating the pair of Acqiris DC-241 digitizers is shown in Fig. 1. Each of the signals was split with the aid of an impedance-balanced passive splitter to feed the inputs of an ORTEC constant-fraction differential discriminator (CFDD), Model 583 and a DC-241 digitizer. The fast signals for feeding the CFDDs were amplified by Hewlett-Packard inverting single-chip amplifiers, Model MSA-0204 with a gain of 11 dB and a frequency range to 1.8 GHz. The blocking-out signals of a rectangular shape with a duration of 50 ns produced by the CFDD units were passively mixed to form an input signal for external triggering the digitizer pair. By a suitable adjustment of the discrimination level an event of triggering could occur only on the onset of overlapping the CFDD blocking-out signals. With this adjustment only the *coinciding* detector signals—i.e. those that were of potential interest—were processed by the digitizers. Further restrictions of the detector signals were imposed by adjusting relatively wide pulse-height windows at the CFDDs to ensure detecting the  $\gamma$ -rays of required energies. Unlike in conventional fast–slow and fast–fast setups the CFDDs served not for precise timing, but for mere reduction of the amount of the accumulated information by excluding a priori uninteresting pairs of the detector signals.

The DC-241 digitizers were working in the master–slave regime, being operated by the Acqiris crate controller, Model CC-103. This regime guaranteed that both digitizers worked ideally in-phase, sharing a common crystal-controlled time-base defined by the clock signals of the master digitizer. Each digitizer included a 512 kB acquisition memory for the temporary storage of the digitized waveforms prior to the transfer of this information to a PC. Technical details regarding the digitizers and the crate controller can be found in Ref. [8].

In our case each waveform was formed by 240 one-byte sample points of a detector signal, with spacing of 250 ps covering a time interval of 60 ns.

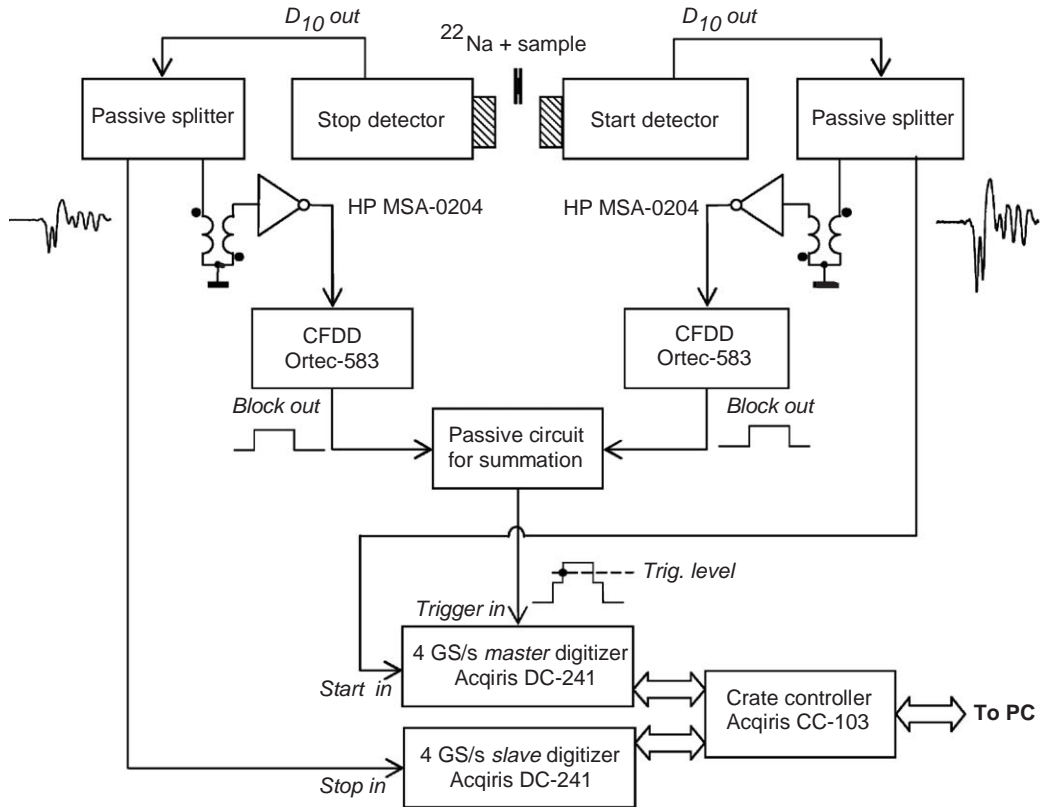


Fig. 1. Block scheme of the setup based on the exploitation of the Acqiris DC-241 digitizers.

The full-scale ranges of the input voltage of the digitizers were adjusted to 200 and 100 mV for the signals from the stop and start detectors, respectively. The transfer of the waveforms to the computer took place repeatedly after acquisition of 200 pairs of waveforms. As the upper limit for the rate of this transfer is about  $100 \text{ MB s}^{-1}$ , the dead time due to the transfer of the waveforms to a PC turned out to be negligible. During the whole run lasting 13.75 h we have accumulated the total number of  $4.2 \times 10^7$  waveform pairs.

For illustration, a set of waveforms, forming one acquisition, is plotted in Fig. 2. The digitized voltage is expressed there in units of the least significant bits (LSBs). A single waveform from the start detector is shown in Fig. 3. Under normal conditions the output signals should be represented by just one positive pulse. However, all the waveforms shown display a rather unexpected

shape: a positive dynode output pulse, going outside the limits of the digitized voltage, is preceded by two parasite, partially separated anode-like negative pulses and followed by strong oscillation. This pathological output signal shape is an artifact of the use of non-standard high-voltage dividers supplying suppressed inter-dynode voltages at the end of the dynode chain and a strongly increased voltage between the first dynode and the photocathode. However, as pointed out in Ref. [5], thanks to the use of these dividers, with our two-detector system we were able to achieve a superior timing resolution power. On these grounds we believe that the leading edge of the first (anode-like) pulse carries the most valuable information regarding the detection time.

The majority of waveforms in Fig. 2 display their minimums approximately at the midpoint of the adjusted 60 ns time range. This is because the

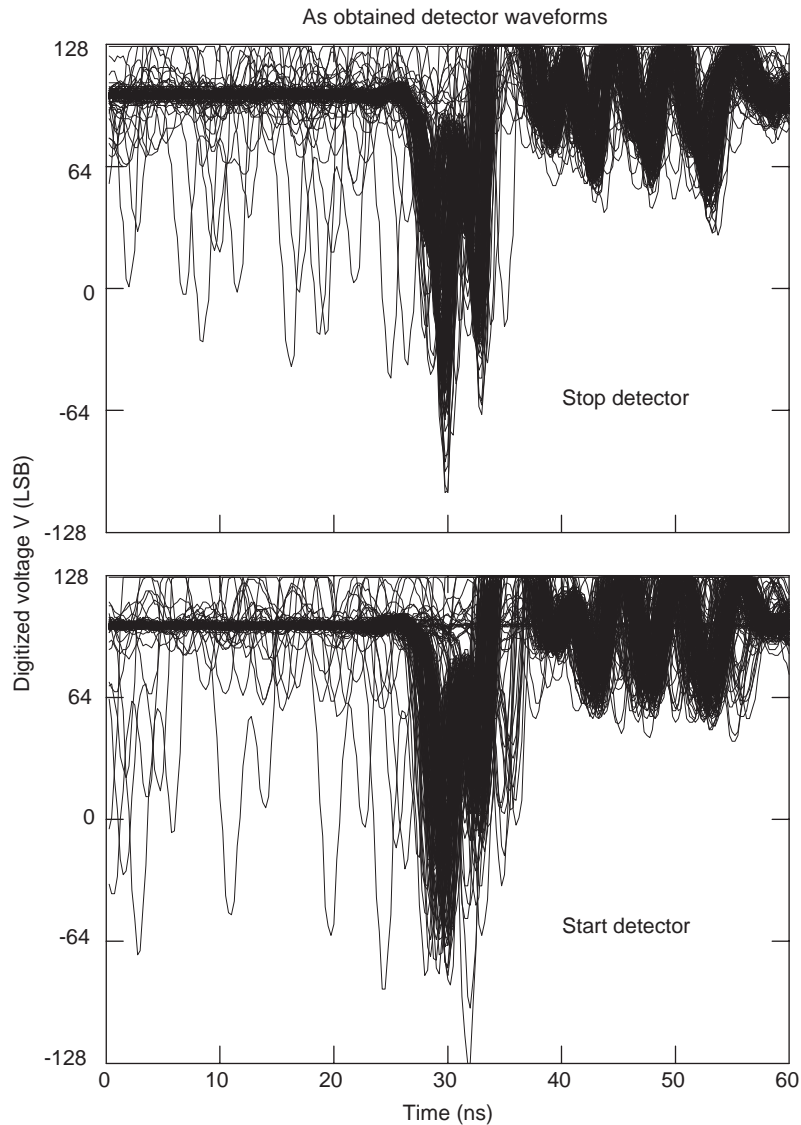


Fig. 2. Two sets of 200 waveforms obtained by sampling the signals from stop and start detectors.

digitizers were intentionally operated in the so-called “50% pre-triggering acquisition regime” [8].

### 3.1.2. Off-line extraction of detection times and accumulating the delayed-coincidence spectra

The accumulated waveform pairs were processed off-line to extract detection times for 511.0 and 1274.6 keV  $\gamma$ -ray pairs belonging to the individual events of positron annihilation. Having a large number of detection-time differences a

delayed-coincidence spectrum could be then constructed and subsequently analyzed with the aim to assess its quality, especially as far as timing resolution power and the makeup of the timing response function were concerned.

The procedure for the extraction of the detection times we applied consists of the steps described below. In this description, for the sake of clarity, we use two terms—the *waveform* and the *signal*. The former stands for a set of sample points

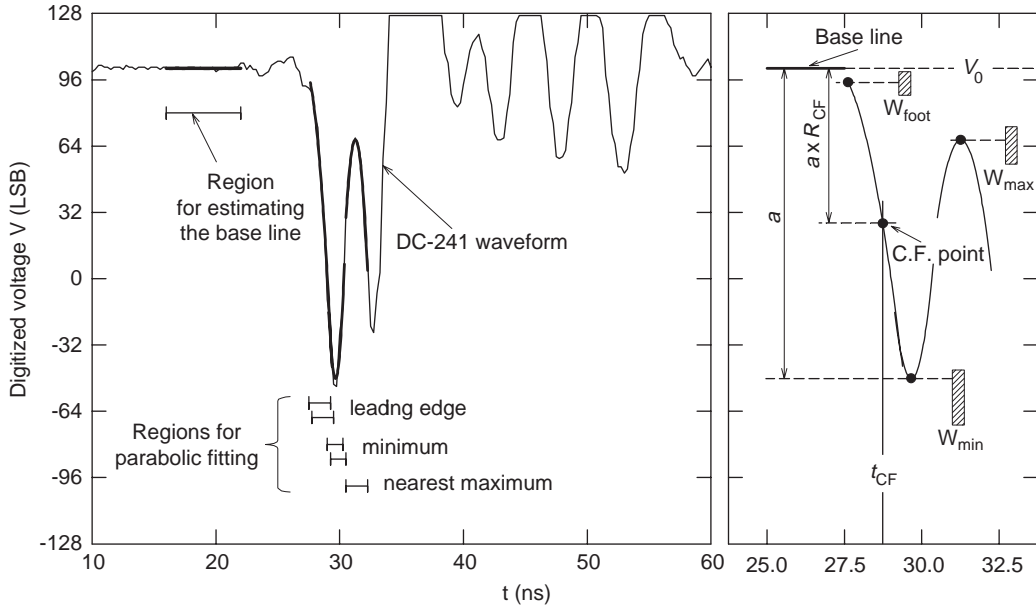


Fig. 3. An example of parabolic approximations of critical sections of a waveform. The right-hand side of this figure elucidates the method for extracting the detection time  $t_{CF}$  by the method of constant fraction.

produced by a digitizer, while the latter—for a real or smoothed detector signal, including its offset.

- (1) A sample point which represents the *absolute* minimum of a given waveform is determined.
- (2) Using a standard parabolic fitting procedure the time and voltage coordinates of the signal minimum are more precisely determined. In fact, this fitting is performed twice, each time using coordinates of a set of 6 consecutive sample points. The first fit is performed using a set in which the point No. 3 is formed by the previously mentioned sample point representing the minimum of the waveform. In the other fit it is the sample point No. 4. The intervals covering these mentioned sextets of sample points are shown in the left panel in Fig. 3. The reason for performing two fits is to minimize a role of a possible even-odd non-uniformity in the distribution of sample points along the time scale. The coordinates of the signal minimum are determined from averaging over coordinates obtained from two parabolic fits. In both panels in Fig. 3 the plotted parabola that approximates the region of the waveform

- minimum represents the average from the outcome of two parabolic fittings.
- (3) In a similar manner, using two regions for parabolic fitting, the leading edge of the most pronounced negative pulse is again approximated by an average parabola. The intervals used for fitting incorporate eight sample points and, as in the previous case, they are shifted from each other by one spacing between the sample points. These intervals are situated at a prefixed distance from the position of the absolute minimum of the waveform. The average leading edge parabola together with the intervals used for fitting are shown in Fig. 3.
- (4) A single parabolic fit is used for the determination of the maximum of the signal that follows immediately after the deepest minimum. The width of the fitted interval is prefixed as well as the relative position of this interval with respect to the position of the absolute minimum of the waveform, see Fig. 3.
- (5) Within a wide enough region that precedes the absolute minimum of the waveform an average value,  $V_0$ , of the signal together with

the root-mean-square deviation (rms) of the signal are estimated. These characteristics are needed for the determination of the position of the baseline and checking its degree of constancy. The average value  $V_0$  thus represents a real-time offset.

- (6) Knowing precise enough absolute minimum of the detector signal and the position of the baseline, the absolute value  $a$  of the amplitude of the anode-like negative pulse is determined.
- (7) In order to accept a given waveform for further analysis, the following conditions are to be satisfied: (i) the rms value of the baseline should be lower than a prefixed value—in our case lower than 2.5 and 1.6 LSB for the signals from the start and stop detectors, respectively; (ii) the initial point of the leading-edge parabola should fall within the prefixed window  $W_{\text{foot}}$ ; (iii) similarly, the absolute minimum and the subsequent maximum, should fall to prefixed windows  $W_{\text{min}}$  and  $W_{\text{max}}$ , respectively, see Fig. 3.
- (8) If the above-outlined conditions are fulfilled, the constant-fraction (CF) method is applied for the determination of the detection time, as illustrated in Fig. 3. Expressing the offset-corrected leading-edge parabola as

$$U(t) \equiv V(t) - V_0 = q_0 + q_1 t + q_2 t^2 \quad (1)$$

the detection time  $t_{\text{CF}}$  is determined as a root of the quadratic equation:

$$U(t) = -aR_{\text{CF}}, \quad (2)$$

where  $R_{\text{CF}}$  is a prefixed CF ratio. For explanation see the right-hand panel of Fig. 3.

- (9) Knowing the co-ordinates of the CF point, a logarithmic derivative of the offset-corrected leading edge at this point is determined

$$\left[ \frac{d}{dt} \ln U(t) \right]_{t=t_{\text{CF}}} = - \frac{q_1 + 2q_2 t_{\text{CF}}}{aR_{\text{CF}}}. \quad (3)$$

If its value is higher than a pre-fixed minimum allowed value, in our case

$$\left[ \frac{d}{dt} \ln U(t) \right]_{t=t_{\text{CF}}} > 1.175 \text{ ns}^{-1}, \quad (4)$$

the deduced detection time  $t_{\text{CF}}$  is accepted for further analysis.

All the steps from 1 to 9 are performed for the waveforms from both detectors. If a waveform pair is not excluded from further analysis in steps 7 and 9, from the detection times deduced the difference  $t_{\text{CF}}^{(\text{stop})} - t_{\text{CF}}^{(\text{start})}$  is calculated and its value is then used for incrementation of the accumulated delayed-coincidence spectrum.

The reason for rejecting the waveforms in steps 7 and 9 is twofold: (i) The condition imposed by the window  $W_{\text{min}}$  provides filtering the waveforms according to the  $\gamma$ -ray energy deposited in the BaF<sub>2</sub> scintillators. This filtering completely excludes all waveforms from the start detector that result from detection of the 511.0 keV  $\gamma$ -rays and suppresses the events of the detection of the 1274.6 keV  $\gamma$ -rays by the stop detector, restricting at the same dynamic range of the accepted detector signals. (ii) The remaining conditions eliminate efficiently a number of those waveform pairs that are damaged by the random pile-up effects caused by uncorrelated events of  $\gamma$ -ray detection. One of the important advantages of the off-line digital processing is a possibility to rule out efficiently the events of pile-up by using several independent digital filters.

A set of 200 pairs of the digitally filtered stop and start waveforms is plotted in Fig. 4. The impact of the filtering is clearly seen from the comparison of the plotted waveforms with those shown in Fig. 2.

In order to accumulate a delayed-coincidence spectrum, the set of  $4.2 \times 10^7$  waveform pairs had to be scanned using the above-specified off-line digital processing. For the sake of getting the delayed-coincidence spectrum of the highest quality, scores of independent scans of the whole set of waveforms had to be undertaken to find optimum adjustments of the parameters governing the regime of the processing. Of particular importance were right adjustments of the CF ratio  $R_{\text{CF}}$ , the widths and positions of windows  $W_{\text{min}}$  and the choice of the optimum region for fitting the leading edge of the waveforms. The histograms in Figs. 5 and 6, deduced from scans Nos. 55 and 57, respectively, represent the best examples of the delayed-coincidence spectra that we obtained. In both these scans the values  $R_{\text{CF}} = 0.50$  and  $R_{\text{CF}} = 0.40$  were adjusted for CF discrimination of the

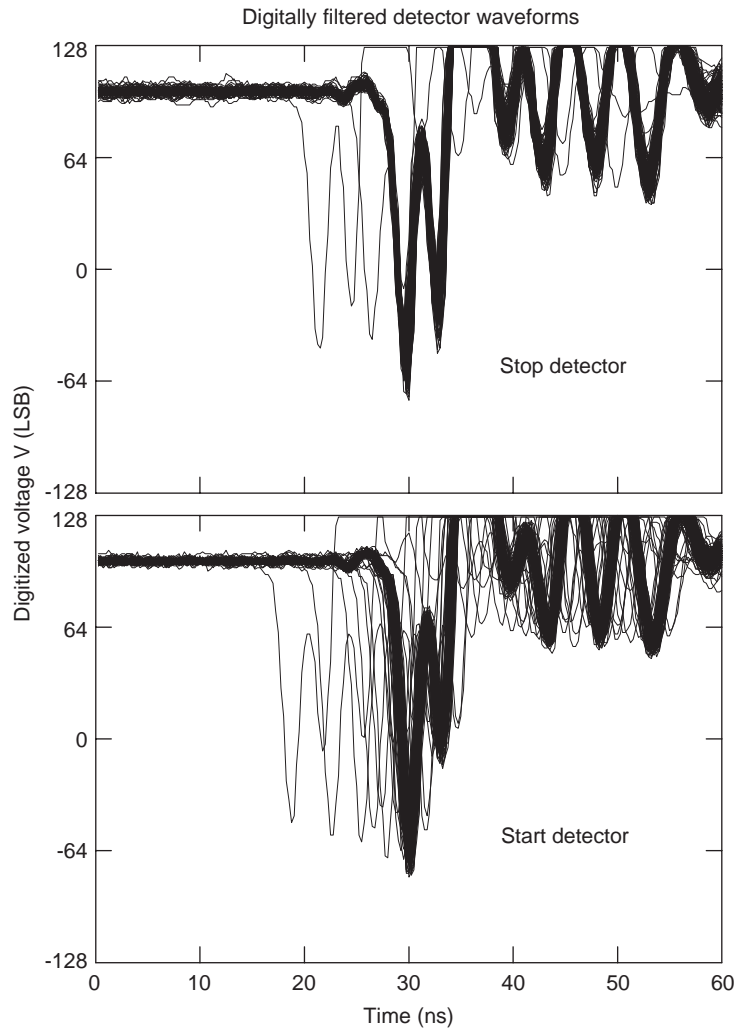


Fig. 4. Two sets of 200 filtered waveforms obtained by sampling the signals from stop and start detectors and the subsequent digital filtering.

stop and start detector signals, respectively. No corrections for a time-zero long-term drift of the delayed-coincidence spectrum were needed because the setup displayed a high degree of long-term stability. It is worth to note that it would be easy to apply these corrections, e.g. with the aid of the method described in Ref. [5]. While scanning the accumulated waveforms we tried to introduce corrections for possible effects of saturation of the detector signals. However, these efforts turned out to be useless, as none of the scans undertaken with various options for these corrections led to any

noticeable improvement of the quality of the resulting delayed-coincidence spectrum.

### 3.1.3. Decomposition of the delayed-coincidence spectra and assessment of the quality of timing response function

From our experience with positron-lifetime spectrometers, based on the use of the BaF<sub>2</sub> scintillation detectors, we found that the timing response functions for these spectrometers are reasonably described by a superposition of three Gaussians differing from each other by their

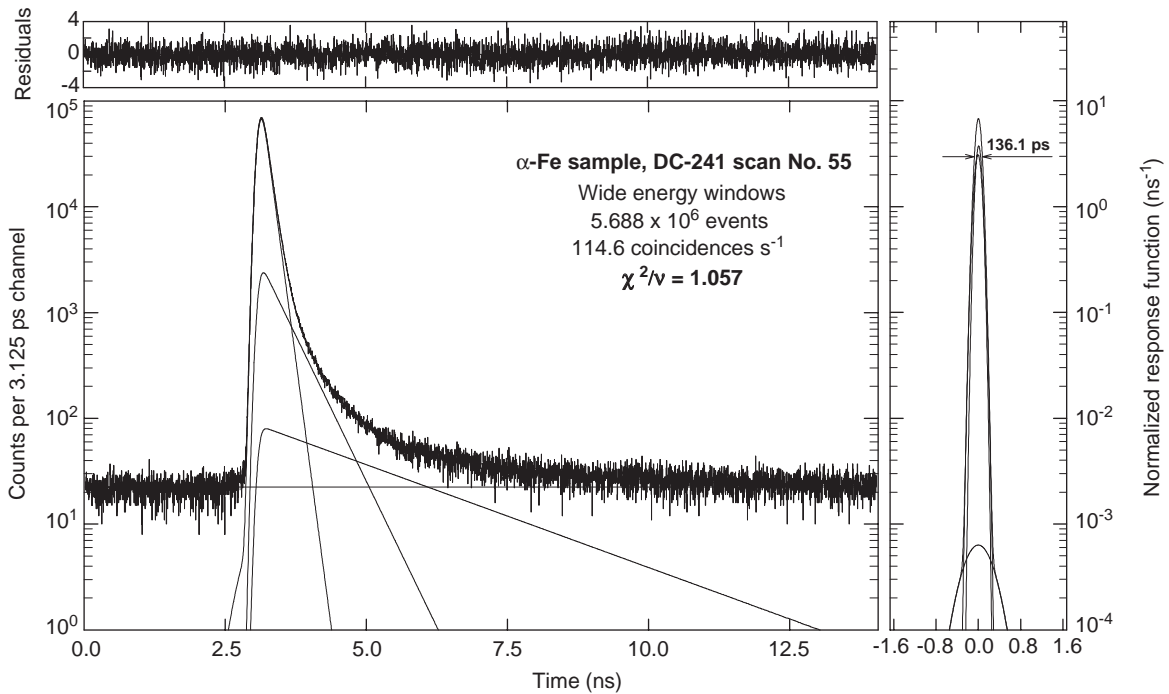


Fig. 5. The largest panel: the delayed-coincidence spectrum obtained from scan No. 55 of the data accumulated from the measurement with the  $^{22}\text{Na}$  source and an  $\alpha\text{-Fe}$  sample using the setup including DC-241 digitizers; the results of the decomposition of the spectrum into contributions of individual positron fractions to the annihilation process are shown. The upper panel: the difference between the experimental spectrum and its fit expressed in units of standard deviation. The panel at the right-hand side: the timing response function deduced and its components.

FWHMs, weights and mutual positions. Within this simple model two of the Gaussians turned out to be relatively narrow and of very close weights, carrying usually about 99.3% or 99.8% of the total area of the response function in the case of the use of fast-fast or fast-slow setups, respectively. The remaining, very weak Gaussian, originating from parasite pile-up effects, were found broad, typically with a FWHM of 500–800 ps. It is also well known that in measurements with a well-annealed  $\alpha\text{-Fe}$  sample only three fractions of positrons are contributing to the delayed-coincidence spectrum: the main fraction, represented by free positrons annihilating in  $\alpha\text{-Fe}$  itself with a lifetime  $\tau = 108.1 \pm 0.2$  ps, see Ref. [5], and the remaining two fractions, representing typically a 6–9% part of the overall area of a delayed-coincidence spectrum. These fractions with lifetimes of 340–420 ps and 1400–2400 ps represent positrons annihilating, respectively, in

the  $^{22}\text{Na}$  source and the organic foils, covering the source.

With this knowledge, using the maximum likelihood method [9], we decomposed both delayed-coincidence spectra obtained from scans Nos. 55 and 57. The results of this decomposition are listed in columns Nos. 2 and 3 of Table 1 and illustrated in Figs. 5 and 6. In the main panels of these figures the fitted components of the spectra that belong to the above-mentioned positron fractions are shown together with a time-independent background resulting from random coincidences. The shown components are represented by exponential functions convoluted with the timing response function, the makeup of which is specified in Table 1 and illustrated on the right-hand side of Figs. 5 and 6. At the upper panels of these figures the residuals of the fits, expressed in units of the standard deviation, are plotted. No traces of imperfect fitting are seen in the behavior of these

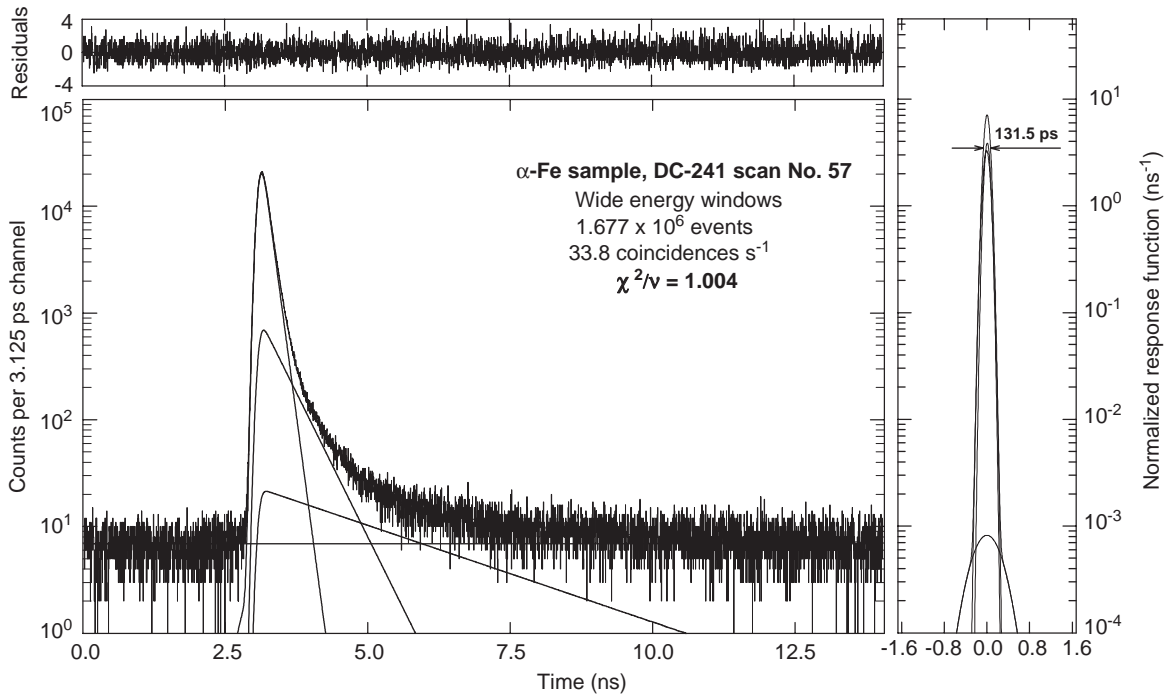


Fig. 6. The delayed-coincidence spectrum obtained from scan No. 57. For explanation see the caption of Fig. 5.

residuals. It is to be stressed that while fitting the spectra, virtually all characteristics responsible for the shape of the overall fit were treated as free parameters, even the distance  $\delta_{1,2}$  between the centroids of two narrow Gaussians of the response functions and the FWHM parameters for all three Gaussians. The only exceptions were the constraint of equality of weights  $G_1$  and  $G_2$  for two narrow Gaussians and the requirement that the position of the third Gaussian of the response function would be the weighted average of the first two. As seen from Figs. 4 and 5, the decomposition of both delayed-coincidence spectra revealed surprisingly low values of the *total* FWHM for the timing response functions, specifically 136.1 and 131.5 ps. As seen from Table 1, the delayed-coincidence spectra from scans No. 55 and 57 yielded the lifetimes for free positrons in  $\alpha$ -Fe equal to  $107.8 \pm 0.3$  and  $108.7 \pm 0.5$  ps, respectively. These results agree well with the above-mentioned expected value of  $108.1 \pm 0.2$  ps for the  $\alpha$ -Fe system.

### 3.2. The reference measurement with the conventional fast-fast setup

In the fast-fast setup employed the signals from the dynode No. 10 of the detectors, described in Section 2, were amplified using the Hewlett-Packard single-chip amplifiers, Model MSA-0204 and led to the inputs of a pair of the ORTEC CFDDs, Model 583. The timing provided by the CFDDs was based on analog-mode processing of the leading, anode-like negative pulse of the detector signal, i.e. the same pulse which was subject to digital processing, as described in Section 3.1.2. The fast timing outputs from the CFDDs served in as start and stop signals for the ORTEC TAC, Model-467 the output of which was led to the input of a Canberra 440 MHz Wilkinson-type ADC, Model-8077. The 14-bit codes at the ADC output from individual events of positron annihilation were immediately transferred to the RAM of a PC where they were used for accumulation of the delayed-coincidence spectrum

Table 1  
Summary of the results from the benchmark testing measurements with two setups for positron-lifetime measurements

Quantity	Setup with DC-241 digitizers		Fast-fast setup
	Scan No. 55	Scan No. 57	
Duration of measurement (h)	13.75	13.75	29.0
Number of coincidences	$5.688 \times 10^6$	$1.667 \times 10^6$	$13.05 \times 10^6$
Energy ranges:			
$\Delta E_{\gamma}^{(\text{stop})}$ (keV)	233	132	
$\Delta E_{\gamma}^{(\text{start})}$ (keV)	510	318	
Lifetimes and intensities:			
$\tau_1^{\text{a}}$ (ps)	$107.8 \pm 0.3$	$108.7 \pm 0.5$	$107.9 \pm 0.2$
$\tau_2$ (ps)	$394.1 \pm 4.9$	$402.9 \pm 4.8$	$368.0^{\text{b}}$
$\tau_3$ (ps)	$2235 \pm 66$	$2398 \pm 136$	$1616 \pm 19$
$I_1^{\text{a}}$ (%)	$91.57 \pm 0.12$	$91.69 \pm 0.21$	$90.99 \pm 0.04$
$I_2$ (%)	$7.33 \pm 0.11$	$7.25 \pm 0.19$	$7.62 \pm 0.05$
$I_3$ (%)	$1.10 \pm 0.02$	$1.06 \pm 0.04$	$1.39 \pm 0.01$
Parameters of response function:			
$\text{FWHM}_1^{\text{c}}$ (ps)	125.3	121.4	155.3
$\text{FWHM}_2^{\text{c}}$ (ps)	151.6	143.3	184.2
$\delta_{1,2}$ (ps)	13.1	13.4	36.2
$\text{FWHM}_3$ (ps)	666.6	651.3	522.7
$G_3$ (%)	$0.045 \pm 0.011$	$0.057 \pm 0.020$	$0.632 \pm 0.033$
$\text{FWHM}_{\text{tot}}$ (ps)	136.1	131.5	173.0
Quality of fit:			
$\chi^2$	4739.9	4502.7	3063.0
$\nu$	4483	4483	2984

The following nomenclature is used: (i)  $\Delta E_{\gamma}^{(\text{stop})}$  and  $\Delta E_{\gamma}^{(\text{start})}$  are the energy width of the windows  $W_{\text{min}}$  for stop and start detector signals; (ii)  $I_i$  and  $\tau_i$  stand for the intensities and lifetimes of three main fractions of annihilating positrons; (iii)  $\text{FWHM}_i$  and  $G_i$  represent the width parameter and the weight for  $i$ th Gaussian component of the timing response function, while  $\delta_{1,2}$  is the separation between the centroids of first two components. For further details see the main text.

<sup>a</sup>For positrons annihilating in  $\alpha$ -Fe.

<sup>b</sup>The lifetime  $\tau_2$  has been fixed at this value during the fitting process.

<sup>c</sup>The weights  $G_1$  and  $G_2$  were assumed to be equal each other, i.e.  $G_1 \equiv G_2 = (100 - G_3)/2$ .

with a channel width of 3.125 ps. Relatively narrow energy windows of the stop and start CFDDs were carefully adjusted at the regions of photopeaks of the 1274.6 and 511.0 keV  $\gamma$ -rays, respectively, to reject those events of annihilation that resulted in detection of the 1274.6 and 511.0 keV  $\gamma$ -rays in not right detectors. Due to this energy discrimination the rate of recorded events of annihilation was reduced to 125 delayed coincidences  $\text{s}^{-1}$ . In order to ensure the best timing resolution, the time delay needed for generating

the analog bipolar signal inside the CFDDs was set at the minimum adjustable value of 0.9 ns. The factory built-in internal CF ratio of the CFDDs was 0.2. A simple, but very efficient software method, described in Ref. [5], was used for real-time compensation of time-zero long-term drift while accumulating the delayed-coincidence spectrum.

During the measurement lasting for 29.0 h a delayed-coincidence spectrum with total area of  $1.305 \times 10^7$  coincidences has been accumulated.

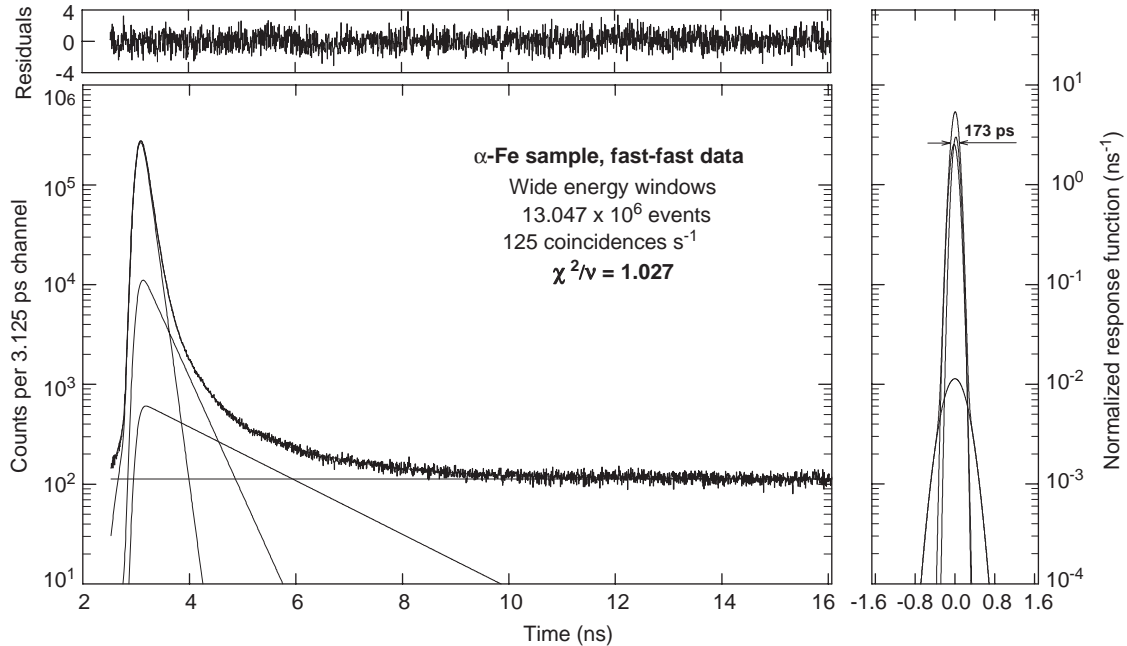


Fig. 7. The delayed-coincidence spectrum obtained from the measurement with  $^{22}\text{Na}$  source and an  $\alpha\text{-Fe}$  sample using the conventional fast–fast setup. For further explanation see the caption of Fig. 5.

The spectrum obtained is shown in Fig. 7. Its decomposition based on the use of the model assumptions formulated in Section 3.1.3 yielded the results summarized in column No. 4 of Table 1 and illustrated in Fig. 7. Although the value of the weighted quadratic deviation  $\chi^2$  in Table 1 indicates an excellent degree of accord between the data and their fit, the plot of residuals in Fig. 7 displays traces of a very small, slowly varying systematic deviation. If this deviation between the experimental and the modeled delayed-coincidence spectrum is statistically significant, it will be probably a price paid for the simplicity of the fast–fast setup. The deduced lifetime of  $107.9 \pm 0.2$  ps attributed to the free positron fraction in  $\alpha\text{-Fe}$  agrees well with the expected value of  $108.1 \pm 0.2$  ps. As seen from Table 1, the width of timing response function found,  $\text{FWHM}_{\text{tot}} = 173.0$  ps, is appreciably higher compared to the values deduced from the measurements with the DC-241 digitizers.

#### 4. Discussion of the results

From the testing measurements with two different setups and the same detector pair it is evident that the use of the ultrafast digitizers for positron-lifetime measurements leads, indeed, to a marked improvement of the quality of the accumulated delayed-coincidence spectra. In particular, compared to the fast–fast setup, the FWHM of the timing response function achieved with the DC-241 digitizers is reduced by a factor of 0.75–0.80. In the case of scan No. 57 the coincidence count rate is virtually equal to that achieved in the measurement with the fast–fast setup.

The measurement with the fast–fast setup is based on an implementation of the CF method and so also the off-line analysis of the data from the setup utilizing the digitizers. However, these implementations are by far not equivalent. In the “digital” implementation the extracted detection

time is represented by the time co-ordinate of the point that lies exactly on the curve of a waveform, the voltage coordinate of this point being equal to  $aR_{CF}$ . However, in the case of pulses displaying shape fluctuations the detection time determined by the “instrumental” implementation of the CF method cannot be rigidly linked to any point that would be positioned at the waveform as specified above. Following our dedicated Monte Carlo simulations<sup>2</sup> it turned out that for realistic detector signals, displaying shape fluctuations, the uncertainty of the detection time obtained by the instrumental implementation of the CF method is appreciably larger compared to the case of the digital CF method. This lead us to believe that the difference in functioning of the digital and instrumental implementations of the CF method is the main reason why the setup utilizing digitizers yielded delayed-coincidence spectra of better quality.

As a result of the stringent digital filtering, the weight of the broad Gaussian component of the response function is suppressed more than by a factor of 10, see Table 1 and Figs. 5–7. The response function achieved is thus virtually free of the parasite contribution from the random pile-up effect. This achievement is an important prerequisite for avoiding hardly controllable errors affecting the deduced lifetimes and intensities of the individual positron fractions. Thanks to the suppression of the effects from the pile-up the residuals plotted in Figs. 5 and 6 do not display any noticeable irregularities within the whole fitted interval of detection-time differences, especially in the narrow region of the leading edge of the delayed-coincidence spectrum which is characteristic by a wide dynamic range of more than three orders of magnitude for the number of recorded events per bin.

As far as the coincidence count rate achieved, it is evident that it can be easily doubled by a simple modification of the algorithm for the extraction of the detection-time difference. Specifically, the modification that abandons the condition that

the waveforms belonging to the 511.0 and 1274.6 keV  $\gamma$ -rays should originate only from fixed detectors, e.g. from detectors Nos. 1 and 2, respectively.

Let us consider a three-detector setup in which the nuclear 1274.6 keV  $\gamma$ -ray and *both* annihilation 511.0 keV  $\gamma$ -rays are detected. The results we achieved led us to believe that with such a setup that would incorporate the DC-241 digitizers and three detectors with timing characteristics equivalent to those of our detector pair, an unprecedented timing resolution power with  $FWMH_{tot} = 105$  ps has to be reached. This judgment is based on the straightforward application of the undisputable law that the uncertainty of the timing of a *single detector* is proportional to  $E_{\gamma}^{-1/2}$ , where  $E_{\gamma}$  is the energy of the detected  $\gamma$ -rays.

## 5. Conclusion

The use of ultra-fast digitizers for positron-lifetime measurements offers unlimited possibilities of off-line processing of the accumulated list-mode data. As demonstrated, the true CF method can be easily applied and carefully optimized for minimizing uncertainties of the extracted detection times. A number of filtering techniques can be used for suppressing the role of pile-up distortions. In addition, with a rate of  $100 \text{ MB s}^{-1}$  for transferring the data from the DC-241 acquisition memory to a computer RAM the role of dead time in positron-lifetime experiments becomes negligible. Last but not the least, a fully programmable amplifier of the DC-241 units is sensitive enough to choose the full-scale range of the input voltage as low as 50 mV. This makes it possible to sample the signals from PMTs working in a regime of a very low current at the end of the active part of the dynode chain, i.e. the regime which may significantly prolong a lifespan of the PMTs.

In spite of the disfavor that the performance of our detectors strongly deteriorated after their long-term use since 1993, the positron-lifetime spectrometer assembled from them and the Acqiris DC-241 digitizers displayed a record timing resolution power. To our knowledge, this setup, based on the traditional concept of detecting the

<sup>2</sup>As the description of these simulations and their results would go beyond the scope of this work it will be included in the paper announced in Section 1.

pairs of 1274.6 and 511.0 keV  $\gamma$ -rays, represents the best positron-lifetime spectrometer of this category. It is to be added that if our detectors had been in such a good shape as in 1993, when timing resolution power of  $\simeq 140$  ps was reached [5], we would have certainly got with them even a substantially better timing resolution than 131 ps.

The timing resolution power achieved with the ultra-fast digitizers is indeed better compared to that obtained using the conventional fast–fast electronics systems. The same conclusion can be made regarding the fast–slow systems as these differ from the fast–fast systems by a not important improvement of timing resolution power at the expense of a sizable drop of the coincidence count rate. This convincingly demonstrates a significant asset of the ultra-fast digitizers for positron-lifetime spectroscopy. We anticipate that with digitizers of the Acqiris DC-241 class in combination with the detectors, formed by BaF<sub>2</sub> crystals and fast PMTs of a new generation or the latest models of the large area multichannel-plate PMTs, the magic resolution barrier of 100 ps will be broken very soon.

### Acknowledgements

It is a pleasure to express our sincere thanks to Mr. Thomas Ornevik and Dr. Allan Rothenberg of Acqiris, SA, Geneva for several helpful discussions and for providing us with a pair DC-241 digitizers for testing measurements. This work was

supported by the Grant Agency of the Czech Republic under Contract GA 106/02/0557 and by the Ministry of Education, Youth and Sports of the Czech Republic under Contract KONTAKT ME 556.

### References

- [1] J. Čížek, I. Procházka, M. Cieslar, R. Kužel, J. Kuriplach, F. Chmelík, I. Stulíková, F. Bečvář, O. Melikhova, R.K. Ismagaliev, *Phys. Rev. B* 65 (2002) 0964106.
- [2] K. Rytšölä, J. Nissilä, K. Kokkonen, A. Laakso, R. Aavikko, K. Saarinen, *Appl. Surf. Sci.* 194 (2002) 260.
- [3] H. Saito, Y. Nagashima, T. Kurihara, T. Hyodo, *Nucl. Instr. and Meth. A* 487 (2002) 612.
- [4] H. Saito, T. Hyodo, *Phys. Rev. Lett.* 90 (2003) 193401  
H. Saito, T. Hyodo, Positron lifetime spectrometer for the measurements of parapositronium lifetime in solids, in: T. Hyodo et al., (Eds.), *Positron Annihilation ICPA-13—Proceedings of the 13th International Conference on Positron Annihilation*, Kyoto, Japan, September 2003, Trans Tech Publications Ltd., Switzerland, Germany, UK, USA, 2004, p. 457.
- [5] F. Bečvář, J. Čížek, L. Lešták, I. Novotný, I. Procházka, F. Šebesta, *Nucl. Instr. and Meth. A* 443 (2000) 557.
- [6] J. Nissilä, K. Rytšölä, K. Saarinen, K. Hautojärvi, *Nucl. Instr. and Meth. A* 481 (2002) 548.
- [7] M. Laval, M. Moszyński, R. Allemand, E. Cormoreche, P. Guinet, R. Odru, J. Vacher, *Nucl. Instr. and Meth.* 206 (1983) 169.
- [8] User Manual—Family of 8-Bit Digitizers, Acqiris, SA, Geneva, 2003; see also web page (<http://www.acqiris.com/Products/Cougar/index.jsp>).
- [9] I. Procházka, I. Novotný, F. Bečvář, *Mater. Sci. Forum* 255–257 (1997) 772.